Research Square

Preprints are preliminary reports that have not undergone peer review.
They should not be considered conclusive, used to inform clinical practice,
or referenced by the media as validated information.

Dynamic connectivity patterns in Parkinson's disease: A new framework for postural control assessment with BioVRSea

Federica Pescaglia
Reykjavik University
Lorena Guerrini
Reykjavik University
Carmine Gelormini
Reykjavik University
Gylfi Thormar
Landspitali University Hospital
Giorgio Di Lorenzo
University of Rome Tor Vergata
Halldór Jónsson Jr
Reykjavik University
Hannes Petersen
Akureyri Hospital
Romain Aubonnet
University of Rome Tor Vergata
Paolo Gargiulo
paolo@ru.is

Reykjavik University

Research Article

Keywords: Parkinson’s disease, Postural control, Electroencephalography, Brain Network States, Virtual reality

Posted Date: August 28th, 2026

DOI: https://doi.org/10.21203/rs.3.rs-10396623/v1

License: This work is licensed under a Creative Commons Attribution 4.0 International License.
Read Full License

Additional Declarations: No competing interests reported.

Dynamic connectivity patterns in Parkinson's disease: A new framework for postural control assessment with BioVRSea

Federica Pescaglia[1], Lorena Guerrini[1,2], Carmine Gelormini[1], Gylfi Örn Thormar[4], Giorgio Di Lorenzo[3,5], Halldór Jónsson Jr[1], Hannes Petersen[7,8], Romain Aubonnet[3†], Paolo Gargiulo[1,9*†]

[1]Institute of Biomedical and Neural Engineering, Reykjavik University, Reykjavik, Iceland.
[2]Department of Mathematics, Physics and Engineering Applications, University of Campania L. Vanvitelli, Caserta, Italy.
[3]Laboratory of Psychophysiology and Cognitive Neuroscience, Department of Systems Medicine, University of Rome Tor Vergata, Rome, Italy.
[4]Department of Neurology, Landspitali University Hospital, Reykjavik, Iceland.
[5]IRCCS Fondazione Santa Lucia, Rome, Italy.
[7]Department of Anatomy, School of Health Sciences, Biochemistry, University of Iceland, Reykjavik, Iceland.
[8]Department of ORL Head and Neck Surgery, Akureyri Hospital, Akureyri, Iceland.
[9]Department of Science, Landspitali University Hospital, Reykjavik, Iceland.

*Corresponding author(s). E-mail(s): paolo@ru.is;
†These authors share last authorship.

Abstract

Purpose: Postural instability is one of the earliest and most disabling features of Parkinson's disease (PD). While previous studies using the BioVRSea paradigm have demonstrated alterations in alpha-band dynamics, the frequency-specific reorganization of large-scale brain networks during postural control (PC) remains

poorly understood. The present study aimed to characterize the dynamic functional connectivity in the delta, theta, and beta bands during a virtual reality (VR) postural task in early-stage PD.
Methods: Twenty early-stage PD patients and twenty-two age-matched healthy controls (CTR) performed the BioVRSea paradigm, which integrates immersive visuomotor stimulation with platform-induced perturbations. EEG source connectivity was estimated using the phase-locking value (PLV), and the resulting connectivity was clustered into recurrent Brain Network States (BNSs) using k-means++. Temporal metrics, including coverage, duration, occurrence, and phase-wise presence, were computed and compared between groups using linear mixed-effects models with FDR correction.
Results: PD patients exhibited a frequency-specific redistribution of BNS dynamics across experimental phases. In the beta band, PD showed reduced coverage (Adjusted p-value=0.004) and duration (Adjusted p-value=0.012) of a DMN-dominant state during baseline in BNS1, alongside increased occurrence (Adjusted p-value=0.032) in BNS2. In the delta band, PD demonstrated an increased occurrence of BNS4 during baseline (Adjusted p-value=0.016), along with a higher percentage of presence across phases, particularly during post-movement recovery, reflecting a persistent, globally synchronized configuration. In the theta band, PD exhibited prolonged BNS4 duration during the pre-movement phase (Adjusted p-value=0.048), accompanied by reduced recruitment of integrative attentional–sensorimotor states during the pre-movement and movement phases.
Conclusion: Early-stage PD is characterized by altered frequency-specific brain network dynamics during PC, reflecting reduced flexibility and abnormal stabilization of large-scale connectivity states. These findings extend previous alpha-band evidence and highlight delta-, theta-, and beta-band BNS metrics as potential neurophysiological biomarkers of early postural dysfunction in PD.

Keywords: Parkinson's disease, Postural control, Electroencephalography, Brain Network States, Virtual reality

Introduction

Parkinson's Disease (PD) is a progressive neurodegenerative disorder characterized by motor symptoms such as bradykinesia, rigidity, and tremor, as well as non-motor manifestations that significantly affect quality of life Tolosa et al. (2006). Among the most disabling features of PD is postural instability, which contributes to falls and reduced autonomy Shumway-Cook and Woollacott (2007); Woollacott and Shumway-Cook (2002). Notably, impairments in postural control (PC) often emerge early in the disease course, even when overt motor symptoms are still subtle. Therefore, identifying sensitive neural markers associated with early-stage postural dysfunction represents a critical challenge for both diagnosis and intervention Kilzheimer et al. (2019).

Electroencephalography (EEG) offers a powerful tool to investigate the neural mechanisms underlying PD due to its high temporal resolution and its ability to capture fast oscillatory dynamics Mulert (2013); Hassan and Wendling (2018); Sakkalis

(2011). While traditional studies have primarily focused on resting-state activity, increasing evidence suggests that task-related EEG provides deeper insight into how the brain dynamically reorganizes under motor and cognitive demands. In particular, oscillatory activity within specific frequency bands has been strongly implicated in motor regulation, attention, and sensorimotor integration, processes that are essential for maintaining balance.

Different frequency bands contribute uniquely to postural and motor control. Delta oscillations (1–4 Hz) are thought to reflect large-scale network coordination and compensatory integration mechanisms, especially during demanding sensorimotor conditions. Theta activity (4–8 Hz) has been linked to cognitive control, attentional engagement, and error monitoring, all of which are crucial for adapting to dynamic perturbations. Beta oscillations (13–30 Hz), tightly linked to motor planning and execution, are particularly relevant in PD, where excessive beta synchronization has been associated with motor rigidity and reduced neural flexibility. Investigating the dynamic reconfiguration of these frequency-specific networks may therefore provide mechanistic insight into the neural alterations underlying postural instability in PD in its early stages (Molcho et al. 2023; Aljalal et al. 2022; Zhang et al. 2022).

To explore these dynamics under ecologically valid yet controlled conditions, we employed the BioVRSea paradigm, a multisensory virtual reality (VR) PC task that integrates visual motion stimulation with synchronized platform-induced perturbations. This setup induces continuous sensory conflict by combining visual flow, vestibular stimulation, and proprioceptive demands, thereby engaging large-scale networks involved in attention, sensorimotor integration, and motor regulation. Unlike traditional laboratory-based balance assessments that rely on static or isolated measures, BioVRSea elicits sustained visuomotor adaptation across distinct experimental phases, enabling the investigation of neural responses during both anticipation and recovery from perturbation Stehle et al. (2022); Aubonnet et al. (2022). BioVRSea represents a critical bridge between controlled laboratory paradigms and ecologically valid balance challenges, offering a sensitive framework to detect early neural dysfunctions before the emergence of clinically evident motor symptoms. By provoking adaptive postural responses within a dynamic and immersive environment, the paradigm allows the characterization of frequency-specific brain network states that may reveal subtle alterations in neural coordination not detectable through conventional behavioral metrics alone.

Recent advances in EEG source connectivity and dynamic network analysis permit the identification of recurring patterns of functional connectivity, referred to as Brain Network States (BNSs) Aubonnet et al. (2023). These transient configurations capture the temporal evolution of large-scale brain organization in response to task demands. Examining BNS dynamics within bands during a complex postural task provides a unique opportunity to investigate how neural flexibility, attentional control, and motor network regulation are altered in PD Petersen and Sporns (2015); Cohen (2015); Tessitore et al. (2014); Lv et al. (2018); Shirer et al. (2012); Raichle (2015); Fox and Raichle (2007).

The present study aims to characterize frequency-specific dynamic functional connectivity in the delta, theta, and beta bands during the BioVRSea PC task, comparing

early-stage PD patients with healthy controls (CTR). In a previous study conducted using the same experimental paradigm, the critical role of alpha-band dynamics over the same cortical regions was highlighted, revealing alterations in network organization associated with PD (Pescaglia et al. 2026). Building upon these findings, the current work extends the investigation to slower (delta, theta) and faster (beta) oscillatory regimes to determine whether complementary or frequency-specific network disruptions characterize early-stage PD.

By analyzing the temporal properties of Brain Network States, including coverage, duration, and occurrence, we aim to identify frequency-dependent biomarkers at the network level associated with impaired postural regulation and early neural dysfunction in this neurodegenerative disease.

Materials and methods

Participants

Participants were enrolled between 18/01/2022 and 03/10/2023 after providing written informed consent. The study was approved by the Icelandic National Bioethics Committee (healthy cohort: *VSN-20–101*; Parkinson's cohort: amendment *VSN-20–101-V2*). A total of 42 individuals took part in the experiment: 20 people with PD (54–82 years, mean age = 65.35) and 22 age-matched CTR (55–72 years, mean age = 62.78). Neither age nor gender differed significantly between the groups, confirming comparable demographic characteristics. Patients were in the early stages of PD and were receiving levodopa. All were assessed in the ON medication state, with no observable motor symptoms during testing. Disease duration at the time of participation was short (approximately 1–2 months post-diagnosis). Disease staging based on the Hoehn and Yahr scale (Bhidayasiri et al. 2012) ranged from 1 to 3. Clinical evaluation indicated that 11 patients had no cognitive deficits, while the others exhibited mild cognitive impairment; none met criteria for Parkinson's dementia. No tremor, dyskinesia, or other involuntary movements were observed during the BioVRSea session. All participants completed the full protocol as well as the pre- and post-experiment questionnaires, which did not indicate any cognitive difficulties.

BioVRSea paradigm

The BioVRSea setup immerses participants in a virtual maritime scene while they stand on a motion platform synchronized with the VR environment. By combining EEG with controlled visuomotor stimulation, the system induces controlled postural challenges and allows assessment of PC. Platform movements amplify the sense of imbalance, especially toward the end of the experiment, prompting participants to engage in stabilizing strategies.

The protocol consists of four sequential phases, as shown in Fig. 1. After an initial baseline (BL) period of two minutes, during which participants stand still while viewing a neutral landscape, the pre-movement phase (PRE) begins with ocean-wave visual stimulation. This is followed by the movement phase (MOV), during which the

platform moves in synchrony with the VR waves, and participants hold a bar for stability. Finally, in the post-movement phase (POST), platform motion stops abruptly while visual motion continues; participants must maintain balance without holding the bar. PRE, MOV, and POST each last 40 seconds, resulting in a total duration of approximately five minutes.

Overall, BioVRSea is designed to probe how the nervous system responds to sensory conflict and dynamic balance demands, particularly by examining changes from the different phases.

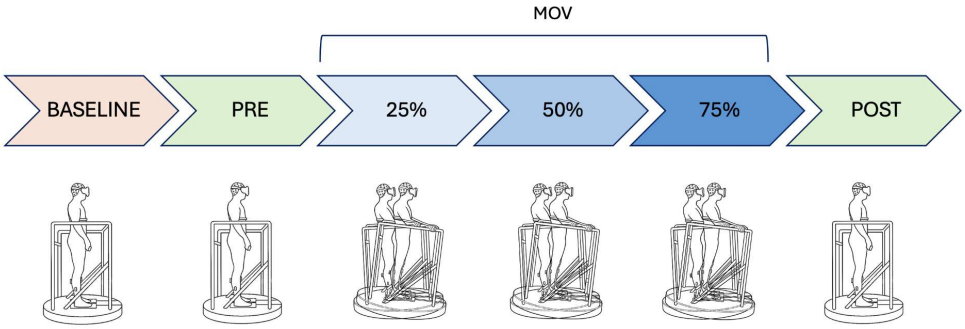


Fig. 1: **Schematic representation of the BioVRSea experimental protocol.** The protocol consists of baseline (BL), pre-phase (PRE), three moving-platform phases corresponding to 25%, 50%, and 75% of the maximal wave amplitude, and post-phase (POST). The moving-platform stimulation phases are collectively referred to as the MOV phase.

Data acquisition

The virtual environment was rendered using software developed by Virtualis (Clapiers, France) and displayed through HTC VIVE VR goggles. EEG was acquired using a 64-channel WaveGuard cap (CA-201; ANT Neuro, Hengelo, Netherlands) at a sampling rate of 4096 Hz. The cap was connected to an ANT Neuro eego amplifier (EE-2XX), which interfaced with a tablet for data recording. The amplifier's very high input impedance (>1 GΩ) and active shielding allow stable measurements even when electrode–scalp impedances are relatively elevated. To optimize contact quality, conductive gel was applied with a blunt syringe, and impedances were kept below 40 kΩ, in line with the manufacturer's recommendations for the device. As reported in ANT Neuro's technical documentation, reliable EEG data can be obtained within this impedance range (ANT Neuro 2023). Furthermore, the pre-processing pipeline effectively mitigates noise arising from impedance variability, ensuring sufficient signal quality for subsequent source reconstruction.

Data pre-processing

Signal pre-processing was performed using the EEGLAB Matlab toolbox to eliminate artifacts, eye blinking, and line noise. Each signal was manually inspected to customize our pipeline. The EEG signals were down-sampled to a frequency of 1024 Hz from the original sampling rate. A dual-filter approach was applied, incorporating a low-pass filter at 1 Hz and a high-pass filter at 45 Hz to enhance signal clarity and diminish noise interference. Channels with flat signals or a correlation coefficient below 60% from neighboring channels were excluded from further analysis as noisy channels. The initial step in artifact removal utilized the Artifact Subspace Reconstruction (ASR) method (Kothe and Jung 2016). Then, independent component analysis (ICA) was performed using the probabilistic ICA for reliable data (PICARD) method (Ablin et al. 2018), known for its effectiveness in handling dynamic recordings. Non-brain components were rejected during this step. Afterward, the previously removed and flat channels were interpolated, while the mastoid electrodes (M1 and M2), along with PO5 and PO6, which measure neck activity, were excluded from the analysis. Finally, the remaining channels (excluding EOG) were interpolated back to 61, and the data were re-referenced to the average.

Data processing: Connectivity analysis and dynamic network computation

The overall methodological pipeline adopted in the present study follows the framework previously validated in (Pescaglia et al. 2026), where detailed descriptions of preprocessing, source reconstruction, dynamic connectivity estimation, clustering procedures, and robustness analyses are provided. The workflow of the present implementation is schematically illustrated in Fig. 2 and adheres to the same validated analytical strategy.

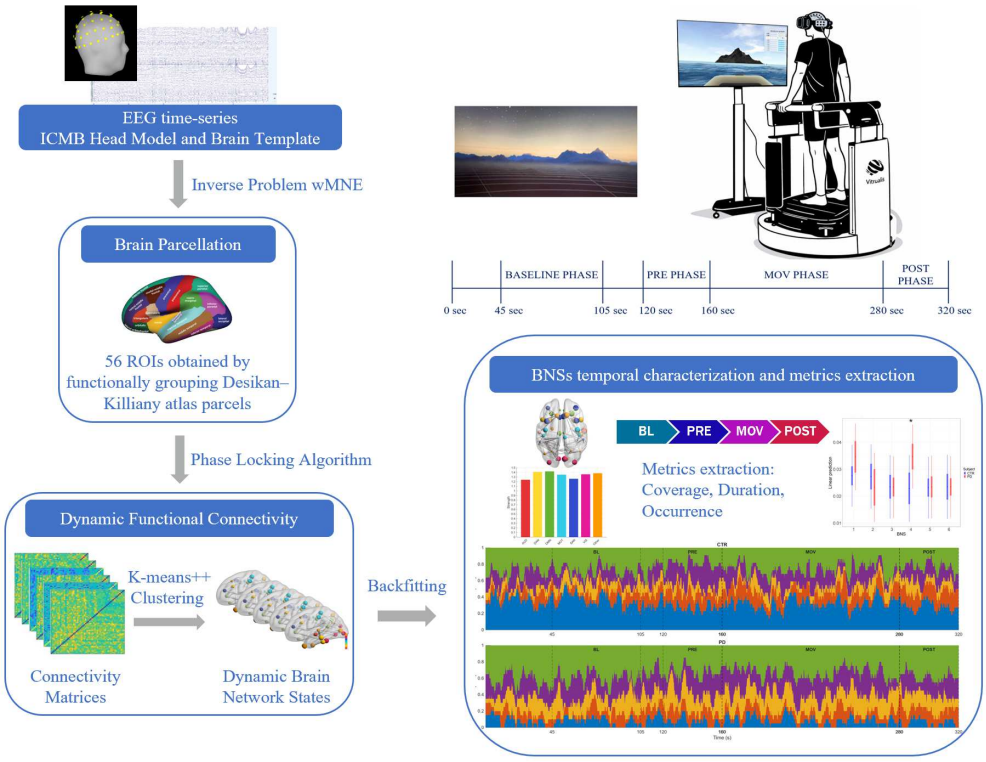


Fig. 2: **Workflow of the BioVRSea analysis pipeline.** EEGs were recorded using 64 electrodes during the BioVRSea experiment. The cortical sources were reconstructed by solving the inverse problem using the wMNE method. After reconstructing the signals based on brain sources, they were reorganized according to 68 brain ROIs of the Desikan-Killiany atlas. Some areas were aggregated to achieve 56 ROIs, aiming for fewer than the 64 total channels. Functional connectivity matrices were computed between the 56 regional time series using the PLV method across the frequency bands: Delta, Theta, and Beta. Connectivity matrices were first obtained separately for the PD and CTR groups, then concatenated before being input into the k-means++ clustering algorithm. This clustering process identified distinct BNSs, followed by network analysis at the subject level to compute metrics for group comparisons.

EEG sensor data were projected into source space using the wMNE solution (Hassan et al. 2014) implemented on a three-layer BEM head model (ICBM template; OpenMEEG). Noise covariance was computed from the first 45 seconds of recording, and source activity from the remaining signal was then parcellated into 56 regions. These ROIs were derived by functionally grouping parcels from the Desikan–Killiany atlas (Desikan et al. 2006) to reduce redundancy, improve source estimation reliability (Farahibozorg et al. 2018; Lopes et al. 2020; Guttmann-Flury et al. 2025), and ensure consistency with the seven canonical Resting State Networks (RSNs) described in previous work (Shirer et al. 2012; Kabbara et al. 2017).

Functional connectivity was estimated between the 56 regional signals using the Phase Locking Value (PLV) (Lachaux et al. 2000) in Beta, Delta, and Theta bands, adopting a sliding-window approach (six-cycle window, 50% overlap). The mathematical formulation is provided in the Supplementary Material **??**. The combination of wMNE and PLV has shown strong performance in capturing meaningful network dynamics during PC and cognitive tasks (Hassan et al. 2014; Aubonnet et al. 2023). This procedure produced a time series of 56×56 PLV matrices for each subject.

For clustering, each connectivity matrix was vectorized by extracting its upper-triangular values, and these vectors were concatenated across all time windows and all individuals. Dynamic Brain Network States (BNSs) were extracted using the modified k-means (k-means++) algorithm (Pascual-Marqui et al. 1995), which is widely applied in EEG and fMRI dynamic connectivity studies (Aubonnet et al. 2024; Zhu et al. 2023; Poulsen et al. 2018).

The number of clusters was determined using a meta-criterion that integrates multiple internal validity indices (Custo et al. 2017; Aubonnet et al. 2024; Mahini et al. 2022). This meta-analysis was performed using the CVIK toolbox (José-García and Gómez-Flores 2023), which aggregates 28 Cluster Validity Indices (e.g., Silhouette, Dunn, Davies–Bouldin, PBM, S_{Dbw}) and several distance measures. The consensus consistently identified the optimal number of clusters. To ensure stability, clustering was repeated with different initialization parameters, and the resulting centroids were compared across runs using Pearson correlation.

Each cluster centroid was then reshaped into a 56×56 connectivity pattern and labeled according to the RSNs contributing most strongly to its topology. The temporal activation of each BNS at the subject level was obtained through back-fitting using Global Map Dissimilarity (Murray et al. 2008; Poulsen et al. 2018), followed by temporal smoothing to remove segments shorter than five windows (Aubonnet et al. 2023).

Following back-fitting, BNS temporal sequences were segmented into the four experimental phases. Within each phase, the presence of each BNS was computed as the proportion of time points assigned to that state relative to the total number of samples in that phase. Subject-level values were then averaged within each group and expressed as percentages for visualization. In addition to this phase-specific characterization, we extracted global BNS-inspired metrics computed over the entire recording, namely coverage, duration, and occurrence rate (Supplementary Material **??**, Tab. **??**). These complementary metrics were used for statistical comparisons between groups to assess differences in both temporal distribution and dynamical stability of brain states.

Data processing: Association of BNSs with RSNs

Each BNS centroid was reshaped into a 56 × 56 symmetric matrix to represent its functional connectivity pattern. Following previous work (Shirer et al. 2012; Kabbara et al. 2017), every node was assigned to one of seven large-scale RSNs: Default Mode Network (DMN), Dorsal Attention Network (DAN), Salience Network (SAN), Motor Network (MOT), Auditory Network (AUD), Visual Network (VIS), or Other. The detailed ROI-to-RSN mapping is provided in Supplementary Material **??**, Tab. **??**.

Node strength was computed using the Brain Connectivity Toolbox (Rubinov and Sporns 2010) as the sum of all weighted connections linked to each ROI. RSN strength was then obtained by aggregating the strengths of nodes belonging to that RSN and normalizing by the number of nodes in the respective network. To determine the dominant RSN of each BNS, we identified networks whose strength exceeded the mean plus one standard deviation across all seven RSNs. Visualization was performed using BrainNet Viewer (Xia et al. 2013), with each ROI colored according to its RSN affiliation and networks displayed using a sparsity threshold of 0.04.

Statistical analysis

The statistical analysis was conducted to investigate the effects of the BNSs and subject group on occurrence, duration, and coverage across different phases of the experimental protocol. The study utilized a linear mixed-effects modeling approach (LMM) to account for the hierarchical structure of the data, where repeated measures within subjects were nested within the levels of the BNSs factor. The primary objective was to ascertain any significant main effects and interactions between the subject group (PD vs. CTR) and the BNSs. Model fit was assessed by examining model summary statistics, including coefficients, standard errors, and p-values derived from likelihood ratio tests. Additionally, an analysis of variance (ANOVA) was performed to assess the overall significance of the fixed effects in the model. To further elucidate significant effects identified by the primary analysis, post-hoc pairwise comparisons were conducted using estimated marginal means. These comparisons aimed to delineate differences in the specific metrics between specific levels of the BNSs factor within each subject group across different experimental phases. To mitigate the risk of Type I errors arising from multiple pairwise comparisons, p-values were adjusted using the Benjamini-Hochberg method. This method controls the False Discovery Rate (FDR) and helps maintain the overall integrity of statistical inference. Results were visualized using empirical cumulative distribution functions and pairs plots to illustrate the distributional properties of the data and highlight significant differences between experimental conditions.

Results

The results are presented for the delta, theta, and beta frequency bands, focusing on the association between BNSs and RSNs, followed by the statistical analysis of BNS temporal metrics. Additional analyses, including time-resolved BNS occupancy descriptive visualizations, phase-wise BNS presence across frequency bands, and detailed spatial characterization of BNSs, are provided in the Supplementary Material (Sections **??** and **??**).

Delta

Association between BNSs and RSNs

BNS1 was characterized by dominant contributions from DAN and SAN, with a distributed topology spanning anterior and posterior regions (Fig. 3, Tab. 1). BNS2

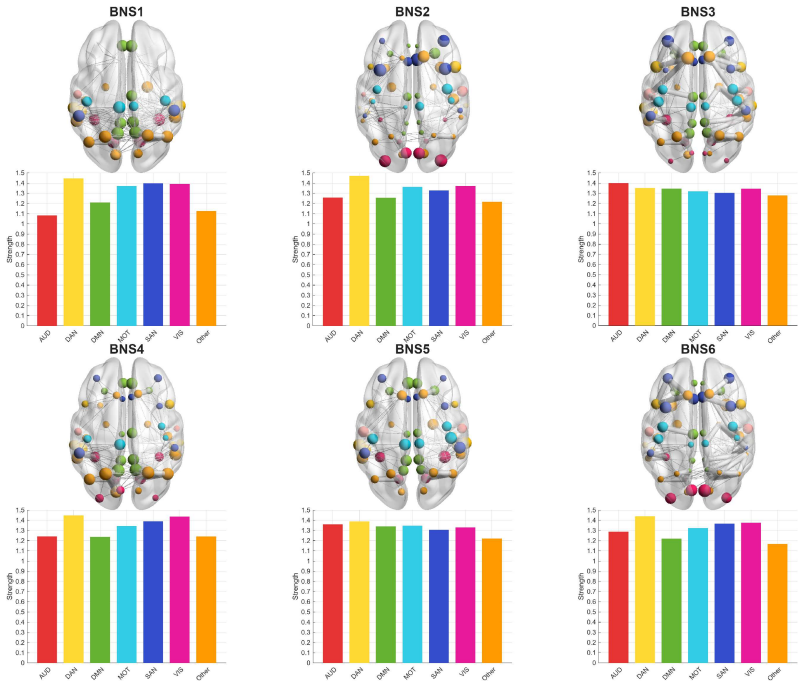


Fig. 3: **Delta: Prevalence of RSNs in each BNS.** Calculated as the sum of the node strength values for each ROI associated with each RSN. Each BNS is displayed with nodes sized proportionally to their strength (sum of incident connection weights), and edges are shown with a sparsity threshold of 0.04 to filter weaker connections. Colors represent distinct RSNs: AUD (red), DAN (yellow), DMN (green), MOT (cyan), SAN (blue), VIS (magenta), Other (orange). This visualization highlights the dominant RSNs contributing to each BNS across experimental phases.

BNS	AUD	DAN	DMN	MOT	SAN	VIS	Other
BNS1	1.083	**1.446**	1.210	1.371	1.399	1.392	1.127
BNS2	1.258	**1.472**	1.257	1.364	1.328	1.372	1.217
BNS3	**1.401**	1.352	1.346	1.319	1.304	1.344	1.280
BNS4	1.243	**1.448**	1.237	1.344	1.390	1.437	1.242
BNS5	1.361	**1.389**	1.341	1.347	1.306	1.331	1.222
BNS6	1.289	**1.439**	1.222	1.324	1.367	1.376	1.168

Table 1: Delta mean strength values for each BNS across networks. The highest value per BNS is highlighted in bold.

showed a DAN-dominant configuration with widespread bilateral distribution across frontal, temporal, and occipital regions (Fig. 3, Tab. 1). BNS3 exhibited a globally integrated profile with relatively balanced contributions across RSNs, including AUD, DAN, and DMN, reflecting a distributed large-scale configuration (Fig. 3, Tab. 1). BNS4 was dominated by DAN and VIS networks, displaying a posterior-centered

topology anchored by midline and occipital regions, consistent with a large-scale attentional–visual integration state (Tab. 1). BNS5 showed a relatively uniform profile across RSNs, with a slight predominance of DAN, indicating a broadly distributed integrative configuration (Fig. 3, Tab. 1). BNS6 was characterized by strong contributions from DAN, SAN, and VIS, with a distributed topology spanning frontal and posterior regions (Fig. 3, Tab. 1).

Statistical analysis of BNSs

To further characterize the temporal expression of these network configurations, we investigated *coverage*, *duration*, and *occurrence* using LMMs with FDR correction. In the *Delta* band, a significant group effect emerged for *Occurrence* in *BNS4* during the *BL* phase, with PD showing higher values than CTR (Fig. 4, Supplementary Material **??**). Notably, BNS4 corresponds to the posterior attentional–visual integration state described above, suggesting that PD patients more frequently engage this large-scale DAN–VIS configuration at baseline.

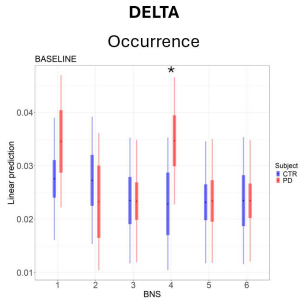


Fig. 4: **LMM analysis.** Linear mixed model analyses revealed significant between-group differences in BNS dynamics. In the *Delta* band, the PD group showed higher *Occurrence* of BNS4 during the BL.

Theta

Association between BNSs and RSNs

BNS1 was dominated by DAN, SAN, and VIS, forming a continuous anterior–posterior organization with strong frontal (DAN–SAN–DMN), central (MOT–DMN–SAN), and posterior (VIS–SAN–Other) interactions, consistent with a large-scale integrative configuration (Fig. 5, Tab. 2). BNS2 showed a relatively uniform profile with slight DAN predominance and widespread connectivity linking frontal, central, and posterior regions, including a prominent right-hemisphere DMN–Other interaction and reduced inferior–posterior coupling. BNS3 exhibited a DAN-dominant and asymmetric organization, with connectivity concentrated in lateral temporal and inferior–posterior regions and sparse superior–central interactions, particularly in the right hemisphere (Fig. 5, Tab. 2). BNS4 reflected a globally integrated, DMN-centered configuration,

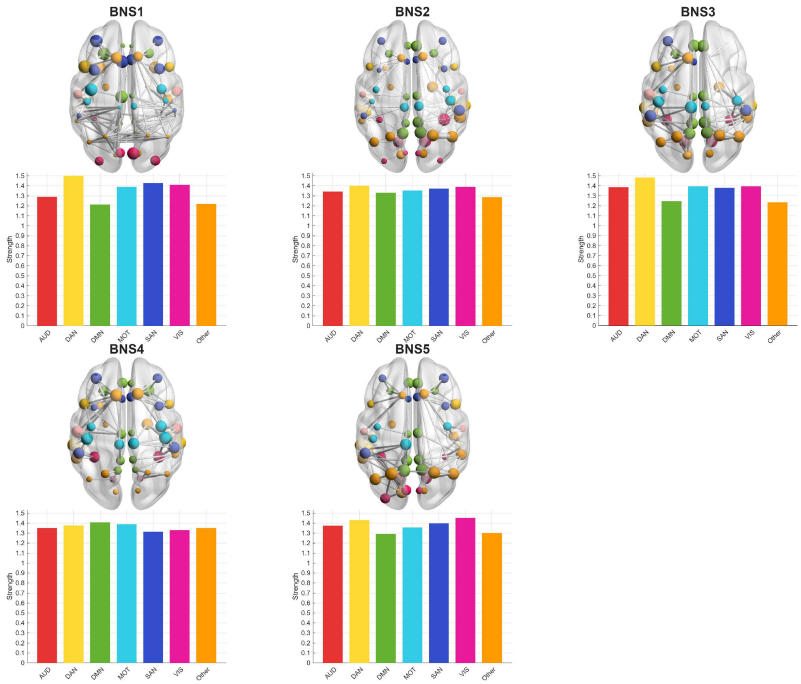


Fig. 5: **Theta: Prevalence of RSNs in each BNS.** Calculated as the sum of the node strength values for each ROI associated with each RSN. Each BNS is displayed with nodes sized proportionally to their strength (sum of incident connection weights), and edges are shown with a sparsity threshold of 0.04 to filter weaker connections. Colors represent distinct RSNs: AUD (red), DAN (yellow), DMN (green), MOT (cyan), SAN (blue), VIS (magenta), Other (orange). This visualization highlights the dominant RSNs contributing to each BNS across experimental phases.

BNS	AUD	DAN	DMN	MOT	SAN	VIS	Other
BNS1	1.291	**1.503**	1.215	1.390	1.429	1.412	1.219
BNS2	1.345	**1.401**	1.332	1.354	1.373	1.391	1.287
BNS3	1.387	**1.484**	1.247	1.395	1.381	1.395	1.236
BNS4	1.351	1.376	**1.408**	1.389	1.314	1.330	1.350
BNS5	1.373	1.431	1.292	1.356	1.397	**1.453**	1.300

Table 2: Theta mean strength values for each BNS across networks. The highest value per BNS is highlighted in bold.

with major hubs in PCC, precuneus, and frontal regions, strongly coupled with motor and attentional systems, forming a large-scale bilaterally symmetric network (Fig. 5, Tab. 2). BNS5 was characterized by VIS–DAN dominance and a right-lateralized anterior-to-posterior connectivity pattern linking frontal, temporal, and posterior occipital regions, consistent with visuospatial integration (Fig. 5, Tab. 2).

Statistical analysis of BNSs

In the *Theta* band, *Duration* in *BNS4* during the *PRE* phase remained significant after FDR correction, with higher values observed in PD compared to CTR (Fig. 6, Supplementary Material **??**). Given that BNS4 reflects a DMN-centered, globally integrated configuration, this result indicates a prolonged engagement of this large-scale default-mode–driven state during the preparatory phase in PD.

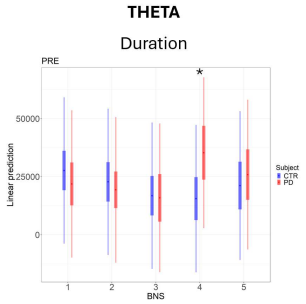


Fig. 6: **LMM analysis.** Linear mixed model analyses revealed significant between-group differences in BNS dynamics. In the *Theta* band, PD exhibited longer *Duration* of BNS4 during the PRE. All reported effects survived FDR correction ($*p < 0.05$)

Beta

Association between BNSs and RSNs

BNS1 showed a globally distributed configuration dominated by DMN and DAN, with strong integration across posterior visual, sensorimotor, and associative regions, forming a largely symmetric large-scale network state (Fig. 7, Tab. 3). BNS2 reflected a DMN-centered integrative state, with prominent midline hubs (PCC, precuneus, ACC) strongly coupled with posterior visual and lateral associative cortices, indicating large-scale interaction between internally oriented and visual systems (Fig. 7, Tab. 3). BNS3 exhibited a relatively balanced configuration with slight DAN–VIS predominance, characterized by posterior and sensorimotor clustering and broadly distributed connectivity, slightly reduced in the right hemisphere (Fig. 7, Tab. 3). BNS4 combined a symmetric sensorimotor core with modest DMN and DAN contributions, including a mild right-lateralized attentional component (Fig. 7, Tab. 3). BNS5 was characterized by strong DAN and AUD contributions, with a predominantly posterior occipital organization and limited involvement of other regions, consistent with a sensory-driven configuration (Fig. 7, Tab. 3).

Statistical analysis of BNSs

In the *Beta* band, significant group differences emerged during the *BL* phase after FDR correction (Fig. 8, Supplementary Material **??**). Specifically, *Coverage* and *Duration* in

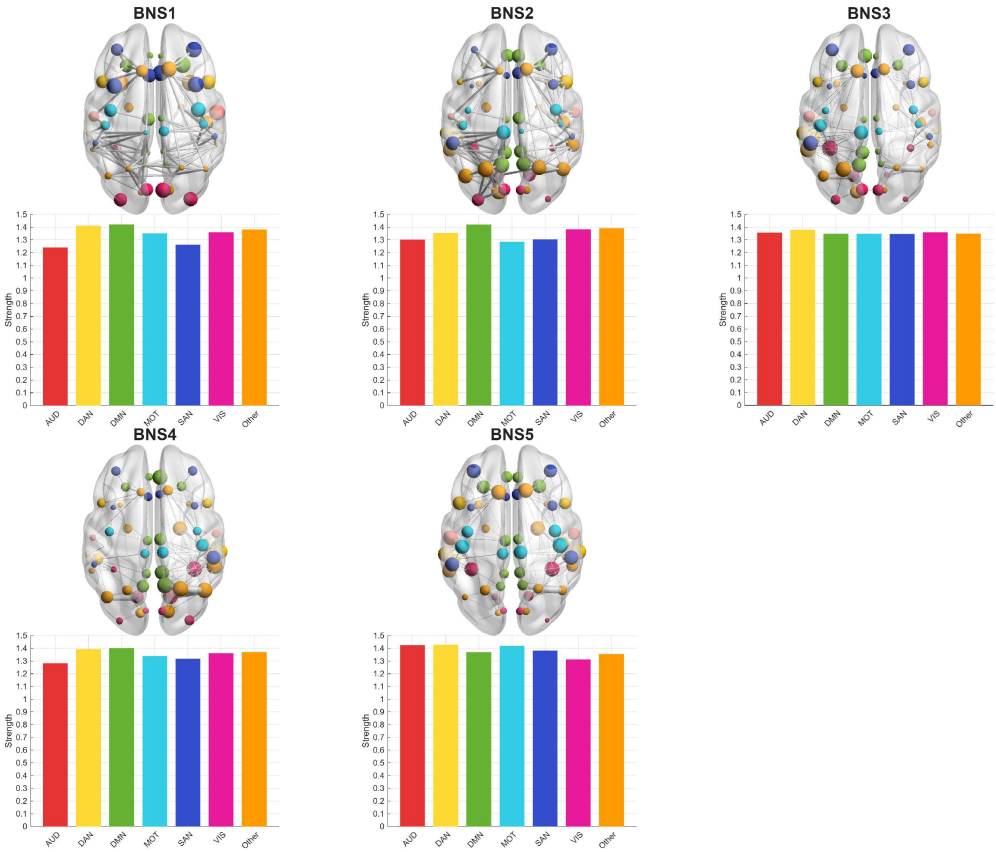


Fig. 7: **Beta: Prevalence of RSNs in each BNS.** Calculated as the sum of the node strength values for each ROI associated with each RSN. Each BNS is displayed with nodes sized proportionally to their strength (sum of incident connection weights), and edges are shown with a sparsity threshold of 0.01 to filter weaker connections. Colors represent distinct RSNs: AUD (red), DAN (yellow), DMN (green), MOT (cyan), SAN (blue), VIS (magenta), Other (orange). This visualization highlights the dominant RSNs contributing to each BNS across experimental phases

BNS	AUD	DAN	DMN	MOT	SAN	VIS	Other
BNS1	1.241	1.412	**1.422**	1.351	1.263	1.360	1.382
BNS2	1.303	1.355	**1.420**	1.286	1.304	1.384	1.391
BNS3	1.358	**1.380**	1.349	1.348	1.347	1.360	1.350
BNS4	1.283	1.393	**1.401**	1.340	1.318	1.363	1.369
BNS5	1.426	**1.428**	1.369	1.418	1.383	1.314	1.355

Table 3: Beta mean strength values for each BNS across networks. The highest value per BNS is highlighted in bold.

BNS1 were higher in controls (CTR > PD), whereas *Occurrence* in *BNS2* was higher in PD patients (PD > CTR).

Notably, BNS1 corresponds to the globally distributed DMN–DAN integrative state described above, indicating a more stable and sustained engagement of this large-scale configuration in controls. In contrast, BNS2 reflects a DMN-centered integrative network linking internal and visual processing systems; its increased occurrence in PD suggests a shift toward more frequent recruitment of this alternative configuration at baseline.

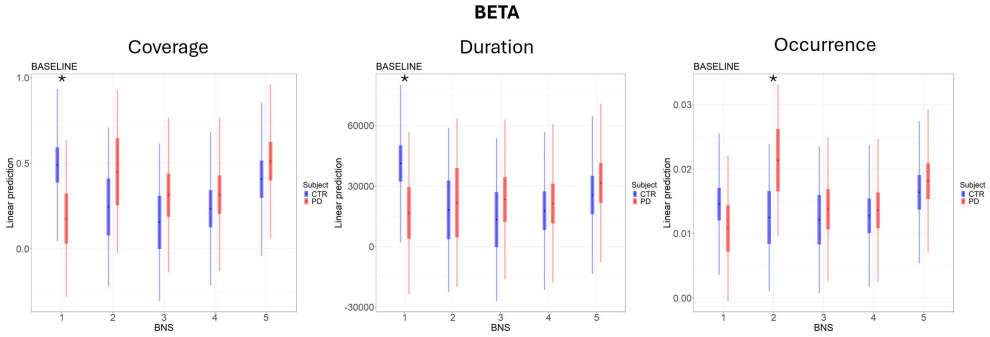


Fig. 8: **LMM analysis.** Group-level LMM analysis in the Beta band during BL revealed distinct differences between PD and CTR groups across Brain Network States. CTR showed higher Coverage and Duration in BNS 1, while PD showed higher Occurrence in BNS 2. All effects remained significant after FDR correction (*$p < 0.05$)

Discussion

This study investigated frequency-specific dynamic brain network states during a complex PC task using the BioVRSea paradigm in patients with early-stage PD. The novelty of this research lies in its visuomotor stimulation approach, which integrates VR and EEG to investigate motor-cognitive interactions in PD under dynamic, ecologically relevant conditions.

To characterize brain network dynamics, we applied a methodological framework adapted from Poulsen et al. for extracting BNSs from functional connectivity data (Poulsen et al. 2018). This pipeline included clustering algorithm selection, BNS optimization, and back-fitting to derive temporal metrics such as coverage, occurrence, and duration (Pescaglia et al. 2026). By applying this approach to EEG connectivity data acquired during the BioVRSea paradigm, we aimed to identify dynamic neurophysiological signatures of PD that may contribute to early disease characterization.

BNSs represent transient configurations of functional connectivity between brain regions. While RSNs describe relatively stable connectivity patterns typically observed during rest, BNSs capture dynamic network configurations that emerge over time across different task conditions. Importantly, many regions contributing to BNSs

belong to canonical RSNs, including default-mode, motor, visual, salience, and attention networks, indicating that these large-scale systems remain functionally relevant during task engagement.

Overall, we identified alterations in delta-, theta-, and beta-band network dynamics in PD compared with CTR. The main finding was that PD was not associated with a simple increase or decrease in connectivity, but rather with a redistribution of brain-state dynamics across frequencies. Specifically, PD showed reduced stability of beta-band integrative states, increased recurrence of slow delta-band attention-dominant configurations, and prolonged theta-band engagement of a DMN-centered state during visually induced self-motion. These findings suggest reduced flexibility in the dynamic reconfiguration of large-scale brain networks during postural control, potentially contributing to the cognitive and motor impairments associated with the disease.

The following sections focus on the BNSs that showed statistically significant between-group differences after linear mixed-effects modeling and FDR correction. Specifically, the main text discusses BNS1 and BNS2 in the beta band, BNS4 in the delta band, and BNS4 in the theta band. The remaining BNSs are not discussed individually in the main text to avoid a purely descriptive state-by-state interpretation; their detailed characterization is reported in the Supplementary Material, Section **??**.

Delta band

Delta-band dynamics revealed a marked reorganization of BNS expression in PD, characterized by increased recurrence of specific slow large-scale configurations and reduced recruitment of others. While CTR showed a more distributed engagement of delta-band states across experimental phases, PD patients exhibited a constrained dynamic repertoire, with greater expression of higher-index states. This redistribution was consistently observed across complementary analyses, including time-resolved occupancy (Supplementary Material **??**), phase-wise presence (Supplementary Material **??**), and temporal metrics, suggesting a robust alteration of slow large-scale coordination mechanisms.

These findings are coherent with the established role of delta oscillations in long-range cortical integration, attentional regulation, and large-scale coordination across distributed brain systems Buzsaki and Draguhn (2004); Buzsáki (2006); Knyazev (2012). In the context of motor control and postural regulation, delta activity has been associated with global network organization, recovery-related processes, and the coordination of distributed sensorimotor and cognitive systems Deco et al. (2011); Bath and Wang (2024). Importantly, increased delta activity and cortical slowing are well-established neurophysiological features of PD, reflecting impaired thalamocortical regulation and large-scale network dysfunction Bosboom et al. (2006); Stoffers et al. (2007); Babiloni et al. (2011). Functional connectivity studies have also reported abnormal delta-band synchronization and disrupted network integration, associated with disease severity, cognitive impairment, and reduced motor adaptability Olde Dubbelink et al. (2014); Voytek and Knight (2015); Kim et al. (2017).

Within this framework, the present findings extend previous spectral observations by showing that delta abnormalities in PD are not limited to global power increases

but are also expressed as alterations in the temporal organization of specific BNSs. In particular, BNS4 showed significantly higher *occurrence* in PD compared with CTR during BL after FDR correction. These results suggest that BNS4 was not merely more prevalent on average, but was also more frequently re-entered in PD, consistent with a fragmented temporal organization of slow network states.

The spatial topology of BNS4 provides a more specific interpretation. In the delta band, BNS4 was primarily DAN-dominant, with strong VIS involvement, and displayed a posterior-centered organization anchored by midline and occipital regions. Medially, prominent hubs included the precuneus (PCUN), posterior cingulate cortex (PCC), and isthmus cingulate (iCC), which were densely interconnected with bilateral occipital associative regions such as the cuneus (CUN), lingual gyrus (LING), fusiform gyrus (FUS), and lateral occipital cortex (LOG). Laterally, strong nodes were evident in temporo-parietal DAN regions (MTG, ITG, pOPER) and parietal associative cortices (IPL, SPL), forming extensive links with occipital and midline hubs (Supplementary Material **??**, Fig. **??**). In contrast, anterior frontal and salience-related regions were present but comparatively less central, suggesting that the functional core of this state was an attention-dominant posterior monitoring configuration rather than an anterior executive state.

Functionally, this anatomy is consistent with a delta-mediated state supporting externally oriented visuospatial integration and sustained attentional monitoring at slow timescales (Buzsaki and Draguhn 2004; Buzsáki 2006; Knyazev 2012). The coupling of occipital associative cortices with PCUN/PCC midline hubs suggests integration between visual processing and medial associative structures, while temporo-parietal DAN nodes indicate top-down attentional allocation over sensory representations. In the context of PC, such a state may reflect reliance on visual-attentional monitoring to stabilize posture and maintain the task set during prolonged standing or recovery.

The increased *occurrence* of this attention-dominant delta state during baseline suggests that PD patients repeatedly entered a monitoring configuration even in the absence of explicit movement demands. This pattern is consistent with cortical slowing and abnormal low-frequency synchronization in PD (Bosboom et al. 2006; Stoffers et al. 2007; Babiloni et al. 2011), as well as with reports of altered large-scale integration/segregation and reduced dynamical flexibility (Olde Dubbelink et al. 2014; Voytek and Knight 2015; Kim et al. 2017). From a dynamical systems perspective, frequent re-entry into BNS4 is compatible with an altered attractor landscape in which specific slow integrative states become easier to access and more repeatedly visited (Deco and Kringelbach 2014; Shine and Poldrack 2018). The elevated occupancy of BNS4 during POST may further suggest impaired recovery dynamics, with PD patients remaining biased toward a posterior monitoring state rather than restoring a broader repertoire of delta configurations after movement.

Theta band

Theta-band dynamics revealed a selective alteration of BNS temporal stability in PD, characterized by prolonged engagement of BNS4 during the PRE phase. Importantly, PRE did not involve mechanical stimulation of the platform, but corresponded to the

visual sea-motion simulation delivered through the VR goggles. During this phase, participants experienced a visually induced sensation of self-motion, as if standing on a moving boat, despite the absence of actual platform displacement. Therefore, the increased duration of BNS4 in PD should be interpreted as a visually driven postural processing effect rather than as a direct motor perturbation.

BNS4 reflected a DMN-centered, globally integrated configuration involving interactions between default-mode, motor, and attentional systems. It was centered on medial DMN hubs, with high nodal strength in the PCC, precuneus, rostral ACC, and orbitofrontal cortex, forming a midline core connected with bilateral motor cortices, including precentral, postcentral, and paracentral regions. DAN regions in lateral temporal areas and posterior visual cortices were also integrated into this network, creating a distributed configuration linking internally oriented, motor, and attentional systems (Supplementary Material **??**, Fig. **??**).

The prolonged duration of this DMN-centered theta state suggests that PD patients remained engaged for longer periods in a large-scale integrative configuration during the processing of visual motion cues. This interpretation is supported by the descriptive occupancy and phase-wise presence analyses, which showed that CTR were mainly characterized by greater expression of BNS1, whereas PD exhibited reduced BNS1 presence and a shift toward BNS2, together with greater contributions from higher-index states, particularly BNS4 and BNS5, across experimental phases (Supplementary Material **??**; Fig. **??**, Tab. **??**). During PRE, PD showed a higher presence of BNS4 and BNS5 than CTR, while CTR showed a greater prevalence of BNS1 and BNS3. Although these supplementary analyses were descriptive, they were coherent with the LMM finding of prolonged BNS4 duration in PD and suggest that theta-band alterations were not limited to a single isolated metric, but reflected a broader tendency toward altered state expression during visually driven postural processing.

This pattern may indicate reduced flexibility in adapting brain network dynamics to sensory conflict, in which visual information suggests body motion while proprioceptive and vestibular inputs do not provide corresponding mechanical perturbation. The persistence of a DMN-centered configuration may reflect increased reliance on internally oriented or compensatory large-scale integration during visually induced postural challenge. Theta oscillations are commonly associated with cognitive-motor integration, attentional control, sensory conflict processing, and adaptive sensorimotor regulation Buzsáki (2006); Klimesch (1999); Sauseng et al. (2010). In balance and postural control paradigms, theta activity has been linked to increased cognitive monitoring and the integration of visual, vestibular, and sensorimotor information under challenging conditions Slobounov et al. (2009); Hülsdünker et al. (2015).

Within this framework, prolonged BNS4 duration during PRE may reflect abnormal stabilization of a theta-band integrative state during visually induced self-motion. Theta activity within medial frontal and cingulate regions has been associated with performance monitoring and control allocation (Cavanagh and Frank 2014); however, excessive persistence of such states may indicate reduced flexibility in switching toward task-optimized configurations. In PD, altered DMN dynamics and impaired segregation between DMN and task-positive networks have been widely reported

(Göttlich et al. 2013; Kim et al. 2017). The increased stability of BNS4 may therefore reflect pathological over-integration between DMN and motor systems, limiting efficient adaptation to visual-motion-driven postural demands.

Beta band

Beta-band dynamics revealed a reorganization of BNS expression in PD, characterized by reduced stability of the dominant configuration observed in CTR and increased recruitment of alternative integrative states. Specifically, CTR showed higher Coverage and Duration of BNS1 during BL, whereas PD showed higher Occurrence of BNS2. Since BNS1 corresponded to a globally distributed DMN–DAN integrative configuration, with strong involvement of posterior visual, sensorimotor, and associative regions, its reduced expression in PD suggests a loss of stable engagement of the main beta-band state observed in controls. Conversely, BNS2 reflected a DMN-centered integrative configuration linking midline default-mode hubs with posterior visual and lateral associative cortices, indicating that PD patients more frequently recruited an alternative state involving internally oriented and visual processing systems.

This interpretation was further supported by descriptive phase-wise presence and time-resolved occupancy analyses. Across phases, CTR maintained a consistent predominance of BNS1, whereas PD showed markedly reduced BNS1 presence and increased expression of higher-index states, particularly BNS3–BNS5 (Supplementary Material **??**; Supplementary Material **??**). Overall, these findings suggest that PD is associated with reduced stability of the dominant beta-band configuration observed in controls and a compensatory or maladaptive shift toward alternative network states. This redistribution may reflect impaired maintenance of an efficient sensorimotor–cognitive set and reduced flexibility in large-scale network coordination. Such an interpretation is coherent with the established role of beta oscillations in stabilizing the current sensorimotor and cognitive state Engel and Fries (2010); Kilavik et al. (2013), as well as with evidence that PD is characterized by abnormal beta-band synchronization and altered beta dynamics related to motor impairment, rigidity of neural processing, and reduced network flexibility Hammond et al. (2007); Little and Brown (2014).

The spatial topology of BNS1 supports its interpretation as a beta-mediated stabilization state. This configuration was characterized by dense bilateral connectivity linking posterior occipital cortices (CUN, LOG, LING, FUS), central sensorimotor regions (preC, postC, paraC), and core DMN hubs (PCC, PCUN, rACC, LOF), with additional DAN contributions (MTG, ITG, pOPER). This posterior–midline–sensorimotor architecture integrated visual feedback, attentional allocation, and motor readiness within a coherent large-scale network backbone (Supplementary Material **??**, Fig. **??**). The significant reduction of both coverage and duration of BNS1 in PD indicates that this integrative posterior–sensorimotor configuration was not only less prevalent but also less temporally stable. Given that beta synchronization in PD is abnormally regulated and excessively rigid at the local level Hammond et al. (2007); Little and Brown (2014), the present findings suggest a complementary large-scale phenomenon: rather than maintaining a coherent distributed stabilization state, PD patients fail to sustain this balanced integrative configuration.

BNS2 displayed a distinct topology centered on midline DMN hubs (PCC, PCUN, ACC), forming a dense medial backbone extending bilaterally toward lateral parietal regions (IPL, SPL), temporal cortices (MTG, STG), and posterior visual–ventral temporal areas (FUS, LOG, LING). Compared with BNS1, sensorimotor regions were less dominant, and the configuration emphasized medial integrative and associative visual–temporal systems. This pattern suggests that BNS2 represents a large-scale integrative state linking internally oriented DMN processing with associative visual and parietal cortices, potentially reflecting monitoring, environmental integration, or transitional cognitive–perceptual processing rather than direct motor stabilization.

The increased occurrence but broadly comparable presence of BNS2 in PD suggests more frequent transitions into this midline-driven configuration, consistent with temporal fragmentation. Importantly, the spatial contrast between BNS1 and BNS2 is revealing: whereas BNS1 tightly couples posterior visual and central sensorimotor cortices with midline hubs, BNS2 emphasizes medial integrative structures with broader associative posterior connectivity and reduced motor dominance. The reduced stability of BNS1, together with increased occurrence of BNS2, suggests that PD shifts beta-band dynamics away from sustained visuomotor stabilization toward more labile midline-integrative states.

BNSs cross-frequency comparison

Taken together, the cross-frequency comparison highlights a convergent alteration of large-scale BNS dynamics in PD, despite the frequency-specific nature of the affected states and temporal metrics (Tab. 4). Across delta, theta, and beta bands, PD-related differences were mainly expressed through abnormal occurrence, duration, or coverage of BNSs dominated by large-scale integrative networks, particularly DAN- and DMN-related configurations. Thus, the common pattern was not the alteration of the same BNS across all frequencies, but rather a shared disruption in the temporal regulation of large-scale brain states.

In the delta band, PD showed increased occurrence of a DAN-dominant BNS4, suggesting repeated recruitment of an attention-related slow integrative state. In the theta band, PD showed prolonged duration of a DMN-centered BNS4 during the PRE phase, when participants experienced visually induced self-motion without mechanical platform displacement. In the beta band, PD showed reduced stability of the dominant CTR configuration, reflected by lower coverage and duration of DMN-dominant BNS1, together with increased occurrence of another DMN-dominant configuration, BNS2. These results indicate that PD alters brain-state dynamics across multiple frequency bands, with each band expressing this alteration through distinct network configurations and temporal properties.

Overall, the shared feature across bands was reduced dynamic flexibility of large-scale brain networks. PD patients appeared less able to maintain or flexibly transition between task-relevant configurations involving attentional, default-mode, sensory, and motor-related systems. This cross-frequency pattern supports the interpretation that postural control impairment in early-stage PD is associated with altered large-scale network reconfiguration, rather than with an isolated abnormality in a single frequency band or resting-state network.

Table 4: Summary of dominant RSN prevalence and significant BNS temporal metrics across frequency bands.

BNS	Delta		Theta		Beta	
	Dominant RSN	**Significant metric**	**Dominant RSN**	**Significant metric**	**Dominant RSN**	**Significant metric**
BNS1	DAN	–	DAN	–	DMN	Coverage CTR > PD; Duration CTR > PD
BNS2	DAN	–	DAN	–	DMN	Occurrence PD > CTR
BNS3	AUD	–	DAN	–	DAN	–
BNS4	DAN	Occurrence PD > CTR	DMN	Duration PD > CTR	DMN	–
BNS5	DAN	–	VIS	–	DAN	–
BNS6	DAN	–	–	–	–	–

Conclusion

The present study demonstrates that early-stage PD is characterized by frequency-specific but convergent alterations in large-scale BNS dynamics during visuomotor postural control. By combining VR-based stimulation with EEG-derived dynamic connectivity analysis, we identified a multiscale reorganization of brain-state expression involving beta, delta, and theta oscillatory regimes. Importantly, PD-related abnormalities were not expressed as a simple increase or decrease in connectivity, but as altered temporal regulation of specific large-scale network states.

In the delta band, PD was characterized by abnormal recurrence of slow, attention-dominant large-scale configurations, particularly the increased occurrence of DAN-dominant BNS4. This suggests repeated recruitment of attentional monitoring states at slow timescales, consistent with reduced flexibility of large-scale network coordination. Rather than reflecting only generalized cortical slowing, delta-band abnormalities were expressed as altered temporal organization of specific BNSs, indicating a biased tendency to re-enter slow integrative states during postural control.

In the theta band, alterations reflected impaired regulation of cognitive–motor and visuospatial processing during visually driven postural challenge. PD patients showed prolonged duration of a DMN-centered globally integrated state, BNS4, during the PRE phase. Importantly, PRE corresponded to the VR sea-motion simulation without mechanical platform displacement, meaning that participants experienced visually induced self-motion and sensory conflict rather than direct motor perturbation. The prolonged persistence of BNS4 therefore suggests reduced flexibility in adapting theta-band network dynamics to visual-motion-driven postural demands, with excessive stabilization of an internally oriented integrative configuration.

In the beta band, PD patients exhibited reduced stability and persistence of the dominant control-like configuration observed in CTR, reflected by lower coverage and duration of BNS1. This state was characterized by a distributed posterior–midline–sensorimotor architecture with strong DMN involvement and broader integration with attentional, visual, and motor-related systems. In parallel, PD showed increased occurrence of BNS2, a DMN-centered integrative configuration linking midline default-mode hubs with posterior visual and associative cortices. Together with the descriptive increase of higher-index states, these findings suggest impaired maintenance of a coherent beta-mediated sensorimotor–cognitive set and a shift toward more labile or compensatory integrative configurations.

Across frequency bands, a coherent systems-level pattern emerged. PD altered both the stability of beta-band sensorimotor–cognitive configurations and the flexibility of slower delta and theta integrative dynamics. The common feature was not the involvement of a single BNS or RSN across all bands, but a frequency-specific disruption of temporal brain-state regulation, involving attentional, default-mode, visual, and motor-related systems.

From a mechanistic perspective, these findings suggest that PD reshapes the large-scale dynamic repertoire of brain activity, reducing adaptive transitions between configurations required for efficient postural control. This multiband reorganization may contribute to impaired motor adaptability, increased reliance on attentional compensation, and reduced automaticity in PD.

Importantly, the integration of VR-based visuomotor stimulation with dynamic BNS analysis provides a sensitive framework for detecting early alterations of brain network flexibility. Frequency-resolved BNS dynamics may therefore represent promising neurophysiological markers of early-stage PD and may inform future biomarker development and intervention strategies targeting network-level dysfunction.

Limitations

Several methodological alternatives exist for both EEG source reconstruction and functional connectivity estimation, and different inverse/connectivity combinations may yield partially different network patterns. In the present study, we adopted the wMNE–PLV pipeline to ensure methodological consistency with previous source-connectivity literature and with earlier BioVRSea investigations, thereby facilitating comparability across studies. Notably, the same analytical framework was previously applied and validated in a study published in *Brain Topography* (Pescaglia et al. 2026), where network dynamics were investigated exclusively in the alpha band. The present work, therefore, represents a systematic extension of that approach, broadening the analysis to additional frequency bands, namely delta, theta, and beta, to characterize band-specific alterations in large-scale brain network states. While our analyses covered theta, delta, and beta bands, gamma-band connectivity was not examined due to the substantially increased computational burden associated with larger and denser connectivity matrices within the current pipeline. Future work will address these aspects by exploring the robustness of the reported results across alternative source localization and connectivity approaches, as well as extending the frequency range to include higher-frequency bands.

Acknowledgments

The authors would like to thank the RANNIS, Icelandic Research Fund (Grant of Excellence no: 239612-051), and the research fund of Landspitali University Hospital.

Author Contributions

Federica Pescaglia: Conceptualization, Data curation, Formal analysis, Investigation, Methodology, Validation, Visualization, Writing – original draft, Writing –

review & editing. Lorena Guerrini: Conceptualization, Data curation, Formal analysis, Investigation, Methodology, Validation, Visualization. Carmine Gelormini: Data curation, Formal analysis, Investigation, Validation, Visualization. Gylfi Örn Thormar: Investigation, Resources. Giorgio Di Lorenzo: Conceptualization, Formal analysis, Methodology, Supervision. Halldór Jónsson Jr: Conceptualization, Formal analysis, Methodology, Supervision. Hannes Petersen: Investigation, Resources. Romain Aubonnet: Conceptualization, Data curation, Formal analysis, Funding acquisition, Investigation, Methodology, Project administration, Resources, Software, Supervision, Validation, Visualization, Writing – original draft, Writing – review & editing. Paolo Gargiulo: Conceptualization, Data curation, Formal analysis, Funding acquisition, Investigation, Methodology, Project administration, Resources, Software, Supervision, Validation, Visualization, Writing – original draft, Writing – review & editing.

Data Availability

The data supporting the findings of this study are not publicly available due to ethical and privacy restrictions related to human participant data. The data are available from the corresponding author upon reasonable request.

Statements and Declarations

Competing interests

The authors declare that there are no conflicts of interest regarding the publication of this paper. None of the authors has any financial or personal relationships that could be perceived as influencing the research outcomes or interpretations presented in this study.

Ethical Approval

All procedures performed in studies involving human participants were in accordance with the ethical standards of the institutional and Icelandic national research committee and with the 1964 Helsinki Declaration and its later amendments or comparable ethical standards. The study protocol was approved by the Icelandic National Bioethics Committee with consent no: VSN-20–101 for the recruitment and assessment of the healthy cohort, and was subsequently extended to include the Parkinson's cohort under amendment no: VSN-20–101-V2.

Informed Consent

All participants received detailed written notification about the study and provided their signed informed consent.

References

Ablin P, Cardoso JF, Gramfort A (2018) Faster ica under orthogonal constraint. In: 2018 IEEE International Conference on Acoustics, Speech and Signal Processing (ICASSP), IEEE, pp 4464–4468

Aljalal M, Aldosari SA, AlSharabi K, et al (2022) Parkinson's disease detection from resting-state eeg signals using common spatial pattern, entropy, and machine learning techniques. Diagnostics 12(5):1033

ANT Neuro (2023) Ant neuro academy faq. https://academy.ant-neuro.com/faq, accessed: 2025-01-17

Aubonnet R, Shoykhet A, Jacob D, et al (2022) Postural control paradigm (BioVRSea): towards a neurophysiological signature. Physiological Measurement 43(11):115002

Aubonnet R, Hassan M, Mheich A, et al (2023) Brain network dynamics in the alpha band during a complex postural control task. Journal of Neural Engineering 20(2):026030

Aubonnet R, Hassan M, Gargiulo P, et al (2024) Dynamic resting-state eeg alpha connectivity: Quantifying brain network state evolution in individuals with psychosis. bioRxiv pp 2024–06

Babiloni C, De Pandis MF, Vecchio F, et al (2011) Cortical sources of resting state electroencephalographic rhythms in parkinson's disease related dementia and alzheimer's disease. Clinical Neurophysiology 122(12):2355–2364

Bath JE, Wang DD (2024) Unraveling the threads of stability: A review of the neurophysiology of postural control in parkinson's disease. Neurotherapeutics 21(3):e00354

Bhidayasiri R, Tarsy D, Bhidayasiri R, et al (2012) Parkinson's disease: Hoehn and yahr scale. Movement disorders: a video atlas: a video atlas pp 4–5

Bosboom J, Stoffers D, Stam C, et al (2006) Resting state oscillatory brain dynamics in parkinson's disease: an meg study. Clinical Neurophysiology 117(11):2521–2531

Buzsáki G (2006) Rhythms of the Brain. Oxford university press

Buzsaki G, Draguhn A (2004) Neuronal oscillations in cortical networks. science 304(5679):1926–1929

Cavanagh JF, Frank MJ (2014) Frontal theta as a mechanism for cognitive control. Trends in cognitive sciences 18(8):414–421

Cohen MX (2015) Effects of time lag and frequency matching on phase-based connectivity. Journal of neuroscience methods 250:137–146

Custo A, Van De Ville D, Wells WM, et al (2017) Electroencephalographic resting-state networks: source localization of microstates. Brain connectivity 7(10):671–682

Deco G, Kringelbach ML (2014) Great expectations: using whole-brain computational connectomics for understanding neuropsychiatric disorders. Neuron 84(5):892–905

Deco G, Jirsa VK, McIntosh AR (2011) Emerging concepts for the dynamical organization of resting-state activity in the brain. Nature reviews neuroscience 12(1):43–56

Desikan RS, Ségonne F, Fischl B, et al (2006) An automated labeling system for subdividing the human cerebral cortex on mri scans into gyral based regions of interest. Neuroimage 31(3):968–980

Engel AK, Fries P (2010) Beta-band oscillations—signalling the status quo? Current opinion in neurobiology 20(2):156–165

Farahibozorg SR, Henson RN, Hauk O (2018) Adaptive cortical parcellations for source reconstructed eeg/meg connectomes. NeuroImage 169:23–45

Fox MD, Raichle ME (2007) Spontaneous fluctuations in brain activity observed with functional magnetic resonance imaging. Nature reviews neuroscience 8(9):700–711

Göttlich M, Münte TF, Heldmann M, et al (2013) Altered resting state brain networks in parkinson's disease. PloS one 8(10):e77336

Guttmann-Flury E, Wei Y, Zhao S, et al (2025) The cost of simplicity: How reducing eeg electrodes affects source localization and bci accuracy. arXiv preprint arXiv:251010770

Hammond C, Bergman H, Brown P (2007) Pathological synchronization in parkinson's disease: networks, models and treatments. Trends in neurosciences 30(7):357–364

Hassan M, Wendling F (2018) Electroencephalography source connectivity: Aiming for high resolution of brain networks in time and space. IEEE Signal Processing Magazine 35(3):81–96. https://doi.org/10.1109/MSP.2017.2777518

Hassan M, Dufor O, Merlet I, et al (2014) EEG source connectivity analysis: from dense array recordings to brain networks. PloS one 9(8):e105041

Hülsdünker T, Mierau A, Neeb C, et al (2015) Cortical processes associated with continuous balance control as revealed by EEG spectral power. Neuroscience letters 592:1–5

José-García A, Gómez-Flores W (2023) Cvik: A matlab-based cluster validity index toolbox for automatic data clustering. SoftwareX 22:101359

Kabbara A, El Falou W, Khalil M, et al (2017) The dynamic functional core network of the human brain at rest. Scientific reports 7(1):2936

Kilavik BE, Zaepffel M, Brovelli A, et al (2013) The ups and downs of beta oscillations in sensorimotor cortex. Experimental neurology 245:15–26

Kilzheimer A, Hentrich T, Burkhardt S, et al (2019) The challenge and opportunity to diagnose parkinson's disease in midlife. Frontiers in Neurology 10:1328

Kim J, Criaud M, Cho SS, et al (2017) Abnormal intrinsic brain functional network dynamics in parkinson's disease. Brain 140(11):2955–2967

Klimesch W (1999) Eeg alpha and theta oscillations reflect cognitive and memory performance: a review and analysis. Brain research reviews 29(2-3):169–195

Knyazev GG (2012) Eeg delta oscillations as a correlate of basic homeostatic and motivational processes. Neuroscience & Biobehavioral Reviews 36(1):677–695

Kothe CAE, Jung TP (2016) Artifact removal techniques with signal reconstruction. 6th International BCI Meeting US Patent App. 14/895,440

Lachaux JP, Rodriguez E, Le Van Quyen M, et al (2000) Studying single-trials of phase synchronous activity in the brain. International Journal of Bifurcation and Chaos 10(10):2429–2439

Little S, Brown P (2014) The functional role of beta oscillations in parkinson's disease. Parkinsonism & related disorders 20:S44–S48

Lopes MA, Junges L, Tait L, et al (2020) Computational modelling in source space from scalp eeg to inform presurgical evaluation of epilepsy. Clinical Neurophysiology 131(1):225–234

Lv H, Wang Z, Tong E, et al (2018) Resting-state functional mri: everything that nonexperts have always wanted to know. American Journal of Neuroradiology 39(8):1390–1399

Mahini R, Xu P, Chen G, et al (2022) Optimal number of clusters by measuring similarity among topographies for spatio-temporal erp analysis. Brain topography 35(5):537–557

Molcho L, Maimon NB, Hezi N, et al (2023) Evaluation of parkinson's disease early diagnosis using single-channel eeg features and auditory cognitive assessment. Frontiers in Neurology 14:1273458

Mulert C (2013) Simultaneous eeg and fmri: towards the characterization of structure and dynamics of brain networks. Dialogues in clinical neuroscience 15(3):381–386

Murray MM, Brunet D, Michel CM (2008) Topographic erp analyses: a step-by-step tutorial review. Brain topography 20(4):249–264

Olde Dubbelink KT, Hillebrand A, Stoffers D, et al (2014) Disrupted brain network topology in parkinson's disease: a longitudinal magnetoencephalography study. Brain 137(1):197–207

Pascual-Marqui RD, Michel CM, Lehmann D (1995) Segmentation of brain electrical activity into microstates: model estimation and validation. IEEE Transactions on Biomedical Engineering 42(7):658–665

Pescaglia F, Guerrini L, Gelormini C, et al (2026) Exploring dynamic alpha band connectivity in parkinson's disease: A novel approach to postural control assessment using the biovrsea paradigm. Brain Topography 39(2):20

Petersen SE, Sporns O (2015) Brain networks and cognitive architectures. Neuron 88(1):207–219

Poulsen AT, Pedroni A, Langer N, et al (2018) Microstate EEGlab toolbox: An introductory guide. BioRxiv p 289850

Raichle ME (2015) The brain's default mode network. Annual review of neuroscience 38:433–447

Rubinov M, Sporns O (2010) Complex network measures of brain connectivity: uses and interpretations. Neuroimage 52(3):1059–1069

Sakkalis V (2011) Review of advanced techniques for the estimation of brain connectivity measured with EEG/MEG. Computers in biology and medicine 41(12):1110–1117

Sauseng P, Griesmayr B, Freunberger R, et al (2010) Control mechanisms in working memory: a possible function of eeg theta oscillations. Neuroscience & Biobehavioral Reviews 34(7):1015–1022

Shine JM, Poldrack RA (2018) Principles of dynamic network reconfiguration across diverse brain states. NeuroImage 180:396–405

Shirer W, Ryali S, Rykhlevskaia E, et al (2012) Decoding subject-driven cognitive states with whole-brain connectivity patterns. Cerebral Cortex 22(1):158–165

Shumway-Cook A, Woollacott MH (2007) Motor control: translating research into clinical practice. Lippincott Williams & Wilkins

Slobounov S, Cao C, Jaiswal N, et al (2009) Neural basis of postural instability identified by vtc and eeg. Experimental brain research 199(1):1–16

Stehle SA, Aubonnet R, Hassan M, et al (2022) Predicting postural control adaptation measuring EEG, EMG, and center of pressure changes: BioVRSea paradigm. Frontiers in Human Neuroscience 16:1038976

Stoffers D, Bosboom J, Deijen J, et al (2007) Slowing of oscillatory brain activity is a stable characteristic of parkinson's disease without dementia. Brain 130(7):1847–1860

Tessitore A, Giordano A, De Micco R, et al (2014) Sensorimotor connectivity in parkinson's disease: the role of functional neuroimaging. Frontiers in neurology 5:180

Tolosa E, Wenning G, Poewe W (2006) The diagnosis of parkinson's disease. The Lancet Neurology 5(1):75–86

Voytek B, Knight RT (2015) Dynamic network communication as a unifying neural basis for cognition, development, aging, and disease. Biological psychiatry 77(12):1089–1097

Woollacott M, Shumway-Cook A (2002) Attention and the control of posture and gait: a review of an emerging area of research. Gait & posture 16(1):1–14

Xia M, Wang J, He Y (2013) Brainnet viewer: a network visualization tool for human brain connectomics. PloS one 8(7):e68910

Zhang W, Han X, Qiu S, et al (2022) Analysis of brain functional network based on eeg signals for early-stage parkinson's disease detection. IEEE Access 10:21347–21358

Zhu Z, Wang H, Bi H, et al (2023) Dynamic functional connectivity changes of resting-state brain network in attention-deficit/hyperactivity disorder. Behavioural Brain Research 437:114121

Supplementary Files

This is a list of supplementary files associated with this preprint. Click to download.

- SupplementaryMaterialDynamicconnectivitypatternsinParkinsonsdiseaseAnewframeworkforposturalcontrolassessmentwithBioVRSea.zip